Thermodynamic Analysis of the System MgO-FeO-SiO_2 at High Pressure and the Structure of the Lowermost Mantle

LARS STIXRUDE[1] AND M.S.T. BUKOWINSKI

Dept. of Geology and Geophysics, University of California at Berkeley

Semi-empirical thermodynamic potentials, based on Debye theory and Birch-Murnaghan finite strain theory are constructed for important mantle phases in the MgO-FeO-SiO_2 system. The parameters are constrained by inverting experimental compression, thermal expansion, thermochemical and phase equilibria data on the relevant phases. Calculated pseudo-unary $MgSiO_3$ and Mg_2SiO_4, and pseudo-binary Mg_2SiO_4-Fe_2SiO_4 phase diagrams agree well with available data. Analysis of the complete ternary system shows that $(Mg,Fe)SiO_3$ perovskite is stable throughout the likely pressure-temperature and compositional regime of the Earth's mantle. The breakdown of perovskite to its constituent oxides is unlikely in the Earth, even at the extreme pressure-temperature conditions of the core-mantle boundary. This reaction had been proposed to reconcile proposed geotherms with predicted silicate melting curves and seismic observations of the deep mantle.

INTRODUCTION

The constitution of the D" layer at the base of the mantle is of broad geophysical interest because the layer is expected to strongly modulate and possibly control the geophysical fields which originate in the Earth's core. The surface manifestations of core heat flow and the geodynamo provide essential information for our understanding of the deep interior and how it affects tectonic, igneous and possibly climatic processes. A significant fraction of core heat may be transported to the surface by mantle plumes that likely originate in D" and are responsible for flood basalts, oceanic plateaus, hot spots and their associated climatic effects [*Duncan and Richards*, 1990; *Tarduno et al.*, 1991]. Possible metallic constituents in D" caused by chemical reaction between mantle and core may distort surface observations of the geomagnetic field, with important implications for models of fluid motion in the core and the geodynamo [*Jeanloz*, 1990]. Correlations between flood basalt activity and geomagnetic field reversal frequency [*Courtillot and Besse*, 1987] as well as arguments based on the secular variation of the magnetic field [*Bloxham and Jackson*, 1991] suggest that lateral and temporal variations in temperature in D", caused by large scale mantle flow, the generation of plumes or the impingement of subducted oceanic crust, may influence the nature of flow in the core and the geodynamo.

The D" layer is a few hundred kilometer thick region of anomalous seismic properties. It is distinguished from the rest of the lower mantle by strong lateral heterogeneity, anomalous, often negative velocity gradients and a velocity discontinuity over much of its upper boundary [*Young and Lay*, 1987; *Weber and Körnig*, 1990]. The mineralogical or compositional changes responsible for these unusual seismic properties remain unknown.

$(Mg,Fe)SiO_3$ perovskite is generally accepted as the most abundant mineral in the lower mantle [*Jeanloz and Knittle*, 1989; *Bukowinski and Wolf*, 1990]. Perovskite dominated assemblages readily account for the seismic properties of the bulk of the lower mantle and phase equilibrium studies over most of the mantle's pressure-temperature regime confirm its stability [*Knittle and Jeanloz*, 1987]. However, the stability of perovskite under D" pressure-temperature conditions has not yet been experimentally addressed.

A comparison of recently proposed geotherms [*Williams and Jeanloz*, 1990; *Knittle and Jeanloz*, 1991b] with predicted silicate melting curves in the deep mantle suggests that perovskite cannot be a constituent of D" [*Stixrude and Bukowinski*, 1990]. Near the core-mantle boundary, its melting point falls more than a thousand degrees below estimated temperatures in the Earth. The proposed core-mantle boundary temperature is primarily determined by the measured melting temperature of iron under shock-loading [*Williams et al.*, 1987] which is found to be significantly higher than model calculations of the iron hugoniot had

[1]Now at School of Earth and Atmospheric Science, Georgia Institute of Technology, Atlanta, Georgia.

Evolution of the Earth and Planets
Geophysical Monograph 74, IUGG Volume 14

predicted [*Brown and McQueen*, 1982]. If the shock wave measurements and the predicted perovskite melting curve are approximately correct, the constitution of D'' must differ substantially from the rest of the mantle, since seismic observations rule out significant amounts of partial melt. If the region's bulk chemistry is dominated, like the rest of the mantle, by Mg, Fe and Si oxide components, perovskite must undergo a transformation to a high pressure phase or assemblage under D'' conditions. A proposed breakdown of perovskite to its constituent oxides permits a solid D'', since oxides are expected to be more refractory than their compounds, and provides a possible explanation of the region's distinctive seismic properties [*Stixrude and Bukowinski*, 1990].

In this report, we present a thermodynamic analysis of the stability of perovskite at high pressures and temperatures and show that the breakdown of perovskite to its constituent oxides is unlikely in the Earth. The reaction does occur at appropriate pressure-temperature conditions but only for iron contents so high that the products disagree severely with the density and bulk modulus of the lowermost mantle. We discuss other possible resolutions of the apparent discrepancy between the perovskite melting curve, the geotherm and seismic observations.

THERMODYNAMIC POTENTIALS

The Gibbs free energy per formula unit, G, of a phase consisting of a solid solution of N species as a function of pressure, P, and temperature, T, is:

$$G_i(P,T)=\sum_{j=1}^{N} x_{ij}[g_{ij}(P,T)+RT\ln a_{ij}] \qquad (1)$$

where x_{ij}, g_{ij} and a_{ij} are the mole fraction, Gibbs free energy and activity of species j in phase i . We assume symmetric regular solution behavior [e.g. *Guggenheim*, 1952]:

$$RT\ln a_{ij}=s_i[RT\ln x_{ij}+W_i(1-x_{ij})^2] \qquad (2)$$

where W_i is the interaction parameter and s_i is the stoichiometric coefficient of the mixing site. The Gibbs free energy is written as: $g_{ij}(P,T)=F_{ij}(V_{ij},T)+PV_{ij}$, where V is the molar volume. We assume that the Helmholtz free energy, F_{ij}, can be divided into a reference term, a purely volume dependent part given by Birch-Murnaghan finite strain theory, a thermal part, given by Debye theory and an electronic contribution, given by free electron theory (subscripts i,j understood) [*Stixrude and Bukowinski*, 1990]:

$$F(V,T)=F_o+F_C(V,T_o)+[F_{TH}(V,T)-F_{TH}(V,T_o)] +[F_{EL}(V,T)-F_{EL}(V,T_o)] \qquad (3)$$

where the subscript o refers to zero pressure and temperature T_o. The cold part is given by:

$$F_C(V)=9K_oV_o[\frac{1}{2}f^2+\frac{1}{3}a_1f^3+\frac{1}{4}a_2f^4\ldots] \qquad (4a)$$

$$f=\frac{1}{2}[(V/V_o)^{-2/3}-1] \qquad (4b)$$

$$a_1=\frac{3}{2}(K_o'-4) \qquad (4c)$$

$$a_2=\frac{3}{2}[K_oK_o''+K_o'(K_o'-7)+143/9] \qquad (4d)$$

where f is the finite strain and K_o and K_o' are the isothermal bulk modulus and its first pressure derivative. Terms of 4th and higher order are unimportant for the phases and pressure ranges considered here and are neglected. In general, the thermal contribution contains both quasiharmonic terms, for which we assume the Debye model, and anharmonic terms [*Wallace*, 1972]:

$$F_{TH}(V,T)=9nRT(T/\theta)^3\int_0^{\theta/T}\ln(1-e^{-t})t^2dt+A_2T^2 \qquad (5)$$

where n is the number of atoms in the formula unit and θ is the Debye temperature, whose negative logarithmic volume derivative is γ, the Grüneisen parameter. Anharmonic terms are expected to be small [*Hardy*, 1980; *Stixrude and Bukowinski*, 1990] at the high pressures of interest here and are neglected (A_2=0). The electronic term appears only for the high pressure form of wüstite (Wü II), which is known to be metallic:

$$F_{EL}=-\frac{1}{2}\beta_o(V/V_o)^{2/3}T^2 \qquad (6)$$

where $\beta_o=(m^*/m)\beta_{FE}$, m^*/m is the free electron mass ratio, which we assume is the same as for Fe and β_{FE} is the free electron heat capacity coefficient, which depends only on zero pressure conduction electron density [e.g. *Ashcroft and Mermin*, 1976]. The structure of Wü II and its solution properties remain unknown. We assume that Wü II forms a complete solid solution with Pe II and that this phase (Mw II) contains an electronic contribution to its free energy even at very small FeO concentrations. These assumptions lead to a lower bound on the free energy of Mw II and thus a lower bound on the width of the perovskite stability field since the structure of Wü II may differ from that of Pe II, and, if a solid solution exists, it is likely insulating or semi-conducting at small FeO contents.

The parameters are either directly measured or constrained by experimental data or first principles calculations (Table 1). Following the approach of *Bass et al.* [1981], we adopt the directly measured value of K_o, where ultrasonic or brillouin determinations exist, and constrain Ko' by inverting compression data. The reference state Debye temperature, θ_o, and Grüneisen parameter, γ_o, are determined by inverting thermal expansion and calorimetric data as described by *Stixrude and Bukowinski* [1990] (see Figures 1-3) [see also *Ita and Stixrude*, 1992; *Hemley et al.*, 1992]. Reference free energies and interaction parameters are

TABLE 1. Thermodynamic potential parameters.

Phase	Formula	V_o (cm^3/mol)	K_o (GPa)		K_o'		θ_o, γ_o		
			Value	Ref.	Value	Ref	θ_o	γ_o	Ref.
Olivine (Ol)	Mg_2SiO_4	43.76	128(2)	1,2	5.0(5)	17	924(10)	1.14(10)	25,26
	Fe_2SiO_4	46.27	127(2)	3	5.2(5)	18	688(10)	1.08(10)	27,28
Wadsleyite (Wa)	Mg_2SiO_4	40.52	174(2)	4	4.0(5)	19	974(10)	1.32(10)	25,29
	Fe_2SiO_4	43.22	174(2)[a]	5	4.0(5)[a]	5	771(50)[c]	1.32(20)[a]	
Spinel (Sp)	Mg_2SiO_4	39.65	183(3)	6	4.1(5)	20	1017(10)	1.21(10)	25,30
	Fe_2SiO_4	42.02	192(3)	7	4.1(5)	21	781(10)	1.21(10)	27,30
Enstatite (En)	$MgSiO_3$	31.33	106(2)	8	5.0(5)	22,23	935(10)	0.97(10)	31,32
Majorite (Mj)	$Mg_4Si_4O_{12}$	114.15	151(10)	9	4(1)[b]		949(50)[d]	1.24(20)[b]	
Ilmenite(Il)	$MgSiO_3$	26.35	212(4)	10	4.3(5)	22	1026(10)	1.48(10)	33
Perovskite (Pv)	$MgSiO_3$	24.46	263(7)	11,12	3.9(5)	11,12	1017(10)	1.96(10)	34,35
	$FeSiO_3$	25.49	263(7)[a]	12	3.9(5)[a]	12	749(50)[d]	1.96(10)[a]	
Magnesio-wüstite (Mw)	MgO	11.25	160(2)	13	4.1(2)	13	776(10)	1.45(10)	26,36
	FeO	12.25	152(2)	14	4.9(2)	14	434(50)[d]	1.45(10)	37
Magnesio-wüstite II (Mw II)	MgO	10.79	161(10)	15	4.1(1.0)	15	698(50)	1.36(20)	15
	FeO	10.84	205(10)	14	6(1)	14	630(50)	1.45(20)[e]	38
Stishovite (St)	SiO_2	14.01	314(8)	16	8.8(8)	24	1152(10)	1.35(10)	27,39
Liquid	Mg_2SiO_4	50.12	37.7(2.0)	41	6.3(5)	23	595(20)	0.99(20)	40,41
Liquid	$MgSiO_3$	38.73	21.3(2.0)	41	6.4(5)	23	625(20)	0.36(20)	40,41

Estimated standard deviations are shown in parentheses. q=2.5(1.7) for perovskite [*Hemley et al.*, 1992] and is assumed to be 1(2) for all other phases. References: 1, *Graham and Barsch* [1969]; 2, *Isaak et al.* [1989]; 3, *Graham et al.* [1988]; 4, *Sawamoto et al.* [1984]; 5, *Hazen et al.* [1990]; 6, *Weidner et al.* [1984]; 7, *Liebermann* [1975]; 8, *Weidner et al.* [1978]; 9, *Bass and Kanzaki* [1990]; 10, *Weidner and Ito* [1985]; 11, *Knittle and Jeanloz* [1987]; 12, *Mao et al.* [1991]; 13, *Jackson and Niesler* [1982]; 14, *Jackson et al.* [1990]; 15, *Bukowinski* [1985]; 16, *Weidner et al.* [1982]; 17, *Olinger* [1977]; 18, *Williams et al.* [1990]; 19, *Fei et al.* [1991b]; 20, *Sawamoto et al.* [1986]; 21, *Bass et al.* [1981]; 22, *Duffy and Anderson* [1989]; 23, *Stixrude and Bukowinski* [1990]; 24, *Tsuchida and Yagi* [1989]; 25, *Ashida et al.* [1987]; 26, *Suzuki* [1975a]; 27, *Watanabe* [1982]; 28, *Suzuki et al.* [1981]; 29, *Suzuki et al.* [1980]; 30, *Suzuki* [1979]; 31, *Krupka et al.* [1985]; 32, *Suzuki* [1975b]; 33, *Ashida et al.* [1988]; 34, *Ito and Takahashi* [1989]; 35, *Knittle et al.* [1986]; 36, *Krupka et al.* [1979]; 37, *Touloukian et al.* [1977]; 38, *Knittle and Jeanloz* [1991]; 39, *Ito et al.* [1974]; 40, *Lange and Carmichael* [1987]; 41, *Stebbins et al.* [1984]. Volumes are from *Jeanloz and Thompson* [1983] except those of Majorite [*Ita and Stixrude*, 1992] and the liquid phases [*Lange and Carmichael*, 1987]. a. Assumed to be the same as the Mg end-member; b. Assumed to be the same as pyrope; c. Dependence on Mg/Fe ratio assumed to be the same as for spinel; d. Ratio of majorite to pyrope thermal debye temperatures assumed to be the same as the ratio of the corresponding elastic debye temperatures.

determined by inverting phase equilibria measurements. We find the set of W_i's and F_{oij}'s which provide the best simultaneous solution to a set of reactions (Table 2) of the form:

$$\sum_{i=1}^{N} \nu_{ij}\mu_{ij}(P_{exp}, T_{exp}, x_{ij\,exp}) = 0 \qquad (7)$$

where μ_{ij}, the chemical potential of species j in phase i:

$$\mu_{ij} = F_{ij} + PV_{ij} + s_i[RT \ln x_{ij} + W_i(1-x_{ij})^2] \qquad (8)$$

is evaluated at the experimentally observed pressure, temperature and mole fraction with the parameters of Table 1. The coefficients, ν_{ij}, balance the reaction. Unary reactions are represented by single P,T points, while each binary reaction includes several observations of the coexisting phases. Because the set of equations (7) depends linearly on the parameters (F_{oij}, W_i) the best least-squares solution is readily found, e.g. by singular value decomposition (Table 3).

The thermodynamic potential (1) is expressed in terms of its natural variables and thus contains all thermodynamic information about the model system; it is a fundamental thermodynamic relation in the terminology of *Callen* [1985]. All thermodynamic properties of the model system are given by pressure and temperature derivatives of (1). The potential formulation has important advantages over alternative schemes which determine G by integrating empirical expressions for the volume and entropy in terms of their conjugate variables (polynomials in pressure and temperature or more complex forms) [see e.g. *Wood and Fraser*, 1977]. Unless self-consistency is explicitly imposed over the temperature and pressure regime of interest, they lead to path dependent results for G and its derivatives. Thermodynamic identities, such as those between mixed partial derivatives:

$$-\left(\frac{\partial S}{\partial P}\right)_T = \left(\frac{\partial V}{\partial T}\right)_P \qquad (9)$$

are everywhere satisfied by our approach, while they are generally not by empirical integration schemes.

In addition to complete self-consistency, the thermodynamic potentials used here generally require only a small number of parameters since they are physically based (finite strain theory and the Debye model of the vibrational density of states), which allows us to constrain each parameter independently by a large number of experimental

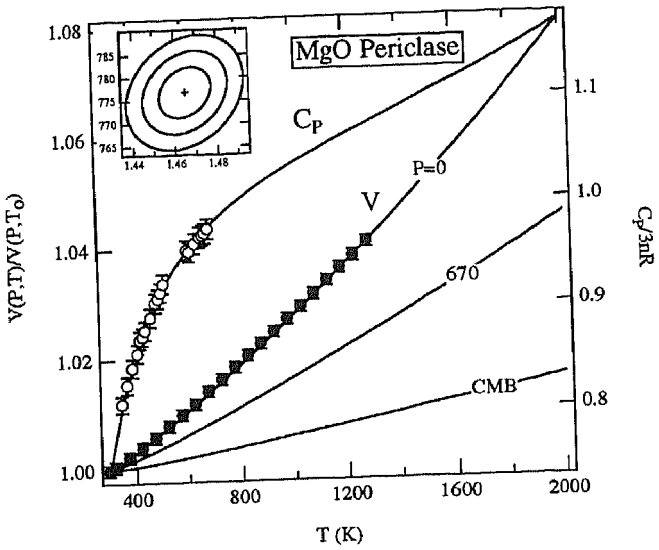

Fig. 1. Inversion of heat capacity and thermal expansion data for the Grüneisen parameter, γ_o, and Debye temperature, θ_o, of Periclase. Lines are calculated using the best fitting parameters, indicated by the cross in the inset (θ_o on the vertical axis and γ_o on the horizontal). The ellipses are 1-, 2- and 3-σ confidence intervals. Thermal expansion at pressures corresponding to the upper mantle-lower mantle boundary (24 GPa), and the core-mantle boundary (136 GPa) is also shown. Sources of the data are given in Table 1.

measurements. The potentials describe a wide variety of thermodynamic properties of mantle minerals at high pressures and temperatures, including their equations of state, phase equilibria and melting behavior [*Stixrude and Bukowinski*, 1990]. In the form of their volume derivative - the Mie-Grüneisen equation of state - they have been extensively tested against shock wave and static compression

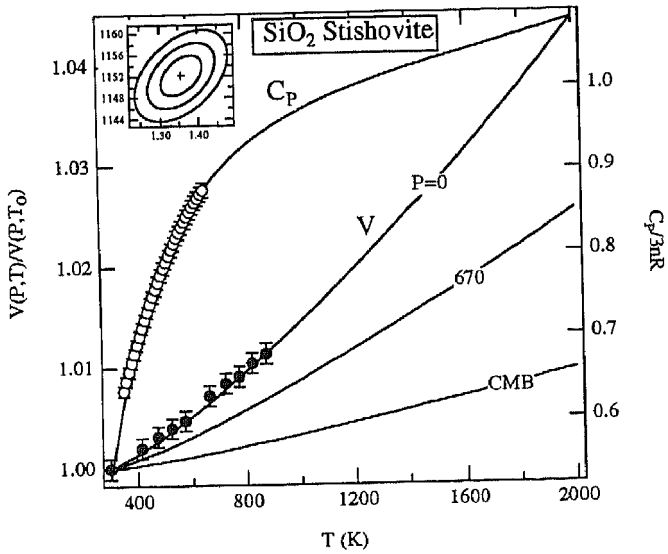

Fig. 2. Inversion of heat capacity and thermal expansion data for γ_o and θ_o of stishovite. The format is the same as in Figure 1.

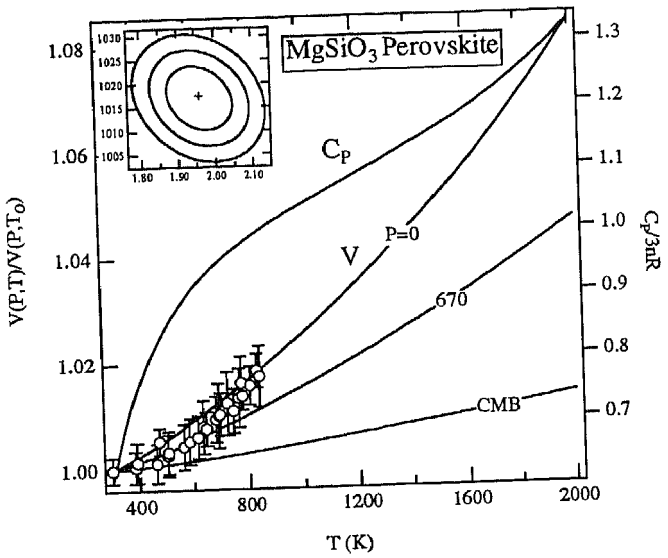

Fig. 3. Inversion of thermal expansion data and experimentally determined dT/dP slopes of the Il=Pv and Sp=Pv+Mw reactions (not shown) for γ_o and θ_o of perovskite. The format is the same as in Figure 1.

data on a wide variety of solids including minerals to lower mantle pressures [*Shapiro and Knopoff*, 1969; *Knopoff and Shapiro*, 1969; *McQueen et al.*, 1970; *Jeanloz*, 1989]. To the extent that anharmonic terms are negligible, the potentials remain sufficiently accurate for our purposes at the extreme

TABLE 2. Reactions used to constrain reference free energies and interaction parameters (Table 2).

Reaction	P (GPa)	T (K)	X_{Fe}	Ref.
Ol=Wa	15.0	1873	0.0	1
Wa=Sp	20.5	1873	0.0	1
Sp=Pv+Mw	24.0	1600	0.0	2
2En=Wa+St	16.1	1573	0.0	3
En=Mj	16.8	1973	0.0	3
2Il=Sp+St	19.5	1273	0.0	3
Il=Pv	22.2	2123	0.0	3
Fo=Liquid	0.0	2163	0.0	4
En=Liquid	0.0	1830	0.0	4
Ol=Sp	6.0	1473	1.0	5
Ol=Sp	12.0	1473	Univ	1
Ol=Sp	13.0	1873	Univ	1
Wa=Sp	12.0	1473	Univ	1
Wa=Sp	13.0	1873	Univ	1
Sp=2Mw+St	22.5-24.5	1373	0.3-0.5	2
Sp=2Mw+St	22-23.1	1873	0.3-0.6	2
Pv=Mw+St	24.5-25.5	1373	0.3-0.4	2
Pv=Mw+St	23-25	1873	0.4-0.5	2

Columns show the pressure and temperature at which the reactions proceed for the indicated bulk iron content (X_{Fe}). For binary reactions, observations over a range of pressure and bulk composition were used. Ol-Wa-Sp binary equilibria were constrained by the observed three phase univariant line. References: 1, *Katsura and Ito* [1989]; 2, *Ito and Takahashi* [1989]; 3, *Gasparik* [1990]; 4, *Stebbins et al.* [1984]; 5, *Akimoto* [1987].

TABLE 3. Thermodynamic potential parameters: reference free energies and interaction parameters. All quantities in kJ/mol.

	Global		High T		Low T	
Species	F_o	W	F_o	W	F_o	W
Forsterite	-127.7	6.1	-133.4	6.3	-124.0	6.5
Fayalite	-93.3	6.1	-96.6	6.3	-89.7	6.5
Mg-Wadsleyite	-99.6	3.9	-105.3	3.9	-95.9	3.9
Fe-Wadsleyite	-98.1	3.9	-100.9	3.9	-93.8	3.9
Mg-Spinel	-92.4	2.8	-98.0	3.6	-88.6	4.1
Fe-Spinel	-94.1	2.8	-97.6	3.6	-90.9	4.1
Mg-Enstatite	-91.0	0	-93.9	0	-89.2	0
Mg-Majorite	-205.4	0	-217.0	0	-198.1	0
Mg-Ilmenite	-35.9	0	-39.0	0	-33.7	0
Mg-Perovskite	3.4	0	-0.4	0	6.6	0
Fe-Perovskite	40.5	0	45.5	0	35.2	0
Periclase	0	13.1	0	13.5	0	12.6
Wüstite	0	13.1	0	13.5	0	12.6
Periclase II	139.7	13.1	139.7	13.1	139.7	13.1
Wüstite II	56.8	13.1	56.8	13.1	56.8	13.1
Stishovite	0	0	0	0	0	0
Mg_2SiO_4 Liquid	-422.9	0	-428.6	0	-419.1	0
$MgSiO_3$ Liquid	-345.6	0	-348.5	0	-343.8	0

pressure-temperature conditions of interest here. The cold part remains well constrained by experimental measurements for most of the relevant phases, while the thermal part closely approaches its high temperature limiting behavior ($T/\theta > 4$). In this limit, results are insensitive to the detailed form of the vibrational density of states which is approximately represented in the Debye model. The adequacy of the regular solution model and the assumed volume dependence of γ is more difficult to evaluate. We ensure that our results are insensitive to wide variations in W and q, the second logarithmic volume derivative of θ.

RESULTS

Predicted pseudo-unary Mg_2SiO_4 and $MgSiO_3$ phase diagrams agree well with the experimentally observed topology and the positions and slopes of the various reactions (Figures 4, 5). The predicted dT/dP slope of the Wa=Sp and Sp=Pv+Pe boundaries are somewhat smaller than observed. The calculated majorite field is smaller than observed. This may be caused by the assumed Debye temperature, which is based on elasticity, or because of the assumption of ideal mixing on the octahedral site. A lower Debye temperature, due perhaps to anomalous vibrational properties of the octahedral site or a favorable interaction between Mg and Si on that site may be responsible for the wider observed stability field. A wider majorite field would also reduce disagreement with the observed melting curve near 16 GPa, which may also be caused by a change in thermodynamic properties of enstatite across the ortho- to clino-enstatite transition which have been ignored here. Because experimental pressure and temperature calibration is difficult under these conditions, differences between calculated and experimental melting curves between 15 and 30 GPa may not be significant. The calculations reproduce both lower and higher pressure measurements [which determine temperature directly, *Knittle and Jeanloz*, 1989a] to within experimental precision.

The predicted topology and temperature dependence of binary Ol-Wa-Sp equilibria also agree well with observation and the position of the univariant lines agree to within .1 GPa (Figures 6, 7). Complete agreement is essentially impossible because the data appear to be mutually inconsistent. At 1473 K observations of coexisting Ol and Wa appear directly above observations of pure Wa near 13.5 GPa, and the observation of Sp at 14.5 GPa is difficult to reconcile with observations of the Wa=Sp end-member reaction. The fact that such inconsistencies are much less frequent in the higher temperature measurements suggests that the lower temperature experiments may not have been sufficiently equilibrated.

Calculated pseudo-binary orthosilicate phase equilibria are compared with the low and high temperature experimental results of *Ito and Takahashi* [1989] in Figures 6 and 7. By

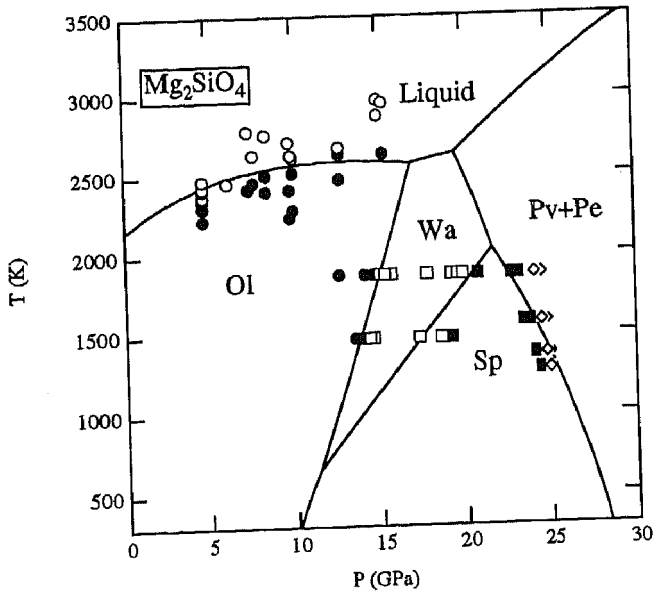

Fig. 4. Calculated pseudo-unary Mg_2SiO_4 phase diagram compared with the experimental data of *Ohtani and Kumazawa*[1981] (Ol=Liquid), *Katsura and Ito* [1989] (Ol=Wa and Wa=Sp) and *Ito and Takahashi* [1989] (Sp=Pv+Pe). For the purposes of illustration we have assumed that the assemblage Pv+Pe melts congruently. Eutectic compositions are expected to lie between orthosilicate and metasilicate stoichiometries at high pressure [*Presnall and Gasparik*, 1989]. Accurate prediction of the eutectic composition requires a multi-component model for the liquid phase, which we do not consider here. Calculated equilibria are identical for the three parameter sets, except for the perovskite forming reactions which are shifted upward and downward by less than 0.5 GPa for the high and low temperature parameters, respectively. Variation of all other parameters within their estimated uncertainties (Table 1) have a smaller effect on calculated equilibria.

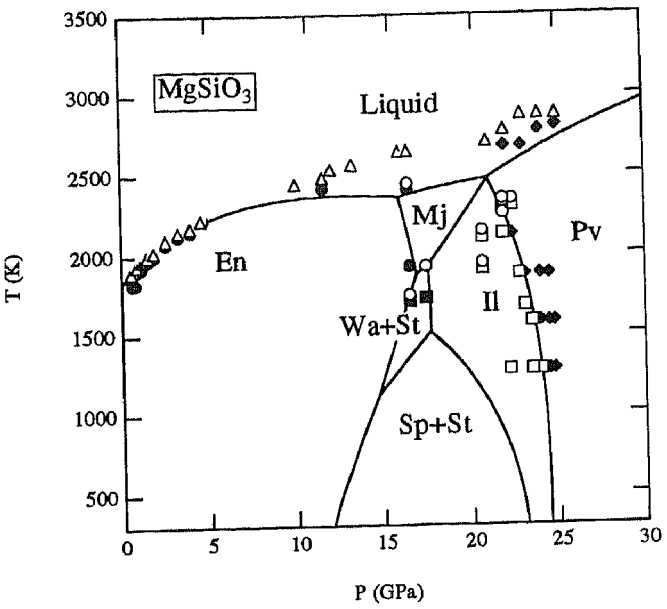

Fig. 5. Calculated pseudo-unary $MgSiO_3$ phase diagram compared with the experimental data of *Boyd et al.* [1964] (melting below 5 GPa), *Presnall and Gasparik* [1990] (melting between 5 and 20 GPa), *Ito and Katsura* [1991] (melting above 20 GPa) *Ito and Takahashi* [1989] (Il=Pv) and *Gasparik* [1990] (subsolidus reactions). Two distinct triple points (Mj=Il=Pv, Mj=Pv=L) appear coincident on this scale. Calculated equilibria are identical for the three parameter sets except for reactions involving Il, which are shifted upward and downward by less than 0.7 GPa for the low and high temperature parameters, respectively. Variation of all other parameters within their estimated uncertainties (Table 1) have a smaller effect on calculated equilibria.

inverting low and high temperature data separately for the reference free energies of the relevant species (Table 3), we obtained excellent fits to the observations. However, it proved impossible to reproduce both experiments with a single set of reference free energies. Parameters which give the best global fit reproduce the general topology but the calculated coexistence loops shift towards more iron rich compositions with decreasing temperature (dashed lines, Figures 6, 7) while the reverse is observed experimentally. The more complex thermodynamic model of *Fei et al.* [1991a] produces very similar results and is also unable to fit the data. The reason for this discrepancy is unclear. Barring severe deficiencies in two very different thermodynamic formulations, insufficient equilibration or an unquenchable phase transition in one or more of the relevant species may be responsible. Despite different predictions for the Pv=Mw+St reaction, all parameter sets produce a very narrow Sp+Pv+Mw coexistence field. This supports the conclusion of *Ito and Takahashi* [1989] that the spinel breakdown reaction can account for seismic reflections at 670 km depth even in a mantle of uniform composition.

Considering the discrepancies apparent in Figures 6 and 7 to be an additional source of uncertainty, the resulting errors in our calculated phase diagrams at D'' pressure -temperature conditions are small and will not affect our basic conclusions. Differences between the predictions of high temperature and global parameter sets are reduced by increasing pressure (Figure 8). The stability field of perovskite is very wide at pressures greater than 60 GPa (1500 km depth), regardless of the parameter set used in the calculations; the low temperature parameters produce an even wider stability field of perovskite.

The predicted high pressure phase diagrams satisfy experimental constraints, including the transition of wüstite to a metallic form, observed near 70 GPa in diamond cell [$T \approx 4000$ K; *Knittle and Jeanloz*, 1986, 1991b] and shock wave experiments [$T \approx 1000$ K; *Jeanloz and Ahrens*, 1980] and perovskite syntheses up to 127 GPa and approximately 2500 K [*Knittle and Jeanloz*, 1987]. Our results closely resemble the predictions of *Jeanloz and Thompson* [1983] below 75 GPa. At higher pressures, our calculations show two pseudo-binary coexistence loops, as required by the phase rule, in place of their four-phase field.

The ternary MgO-FeO-SiO_2 diagram summarizes the

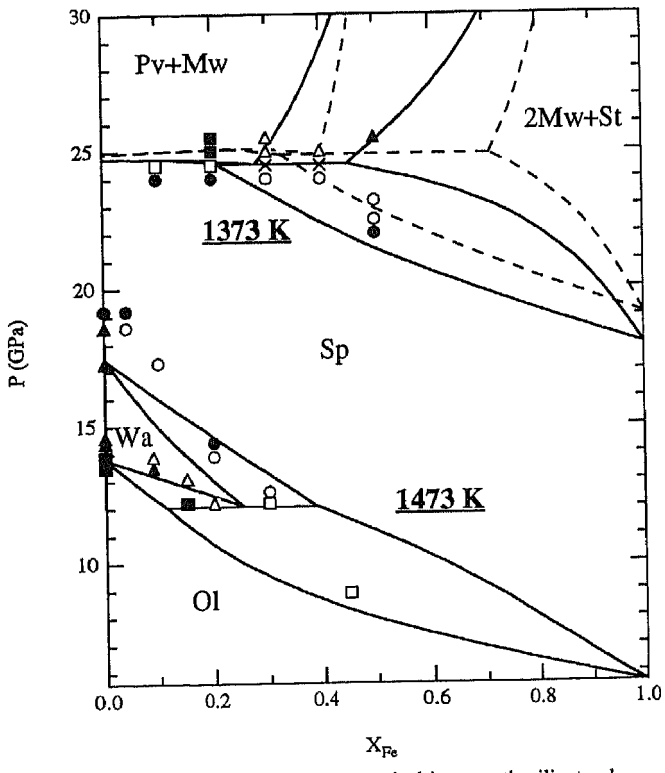

Fig. 6. Low temperature calculated pseudo-binary orthosilicate phase diagram compared with the experimental data of *Katsura and Ito* [1989] and *Ito and Takahashi* [1989]. Closed and open symbols and crosses represent observations of pseudo-unary, -binary, and -ternary coexistence. Solid lines are calculated with the low temperature parameter set, dashed lines with the global parameter set. The Ol-Wa-Sp equilibria differ by less than 0.02 X_{Fe} units for the three parameter sets.

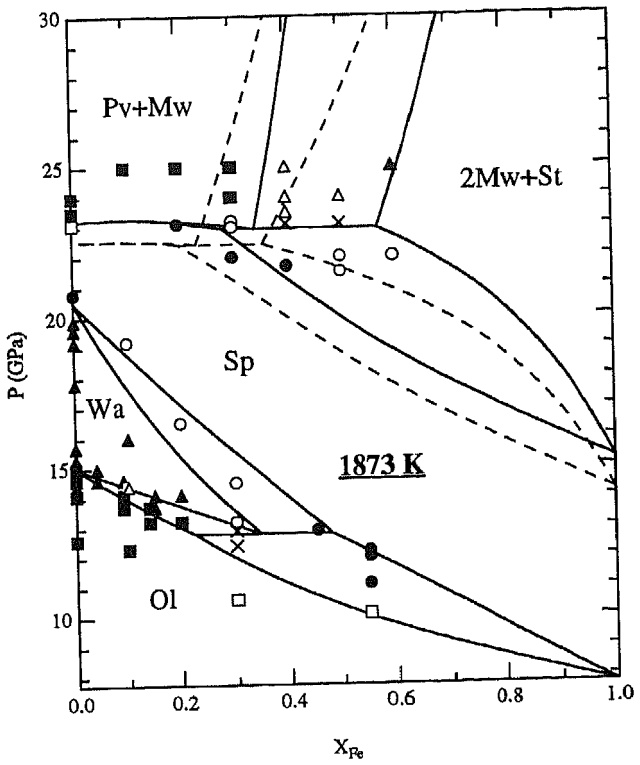

Fig. 7. High temperature calculated pseudo-binary orthosilicate phase diagram compared with the experimental data of *Katsura and Ito* [1989] and *Ito and Takahashi* [1989]. Closed and open symbols and crosses represent observations of pseudo-unary, -binary, and -ternary coexistence. Solid lines are calculated with the high temperature parameter set, dashed lines with the global parameter set. The Ol-Wa-Sp equilibria differ by less than 0.02 X_{Fe} units for the three parameter sets. Variations in all other parameters within their estimated uncertainties (Table 1) have a smaller affect on calculated equilibria.

important results (Figure 9). To obtain a conservative estimate of the stability of perovskite with respect to its constituent oxides in D", we have chosen an extreme temperature [5000 K, higher than the melting point of perovskite at this pressure; *Stixrude and Bukowinski*, 1990] since lower values widen the perovskite stability field. Superimposed on the phase diagram are contours of density and bulk modulus calculated with the same thermodynamic potential formalism and the same parameters used to determine the phase diagram. The intersection of the contours corresponding to the observed density and bulk modulus at the base of the mantle [*Dziewonski and Anderson*, 1981], which represent the location of the Earth at this pressure, lies well within the stability field of perovskite.

The uncertainties in seismic properties near the core mantle boundary are larger than those in the rest of the mantle but correspond to an area of the phase diagram much smaller than that of the perovskite stability field (a Backus-Gilbert resolution calculation using an improved free-oscillation data set indicates that the density and bulk modulus averaged over the entire D" layer are uncertain by approximately 1 %; G. Masters, personal communication, 1992). Uncertainties in the calculations are also much too small to substantially alter the phase diagram. Variations in experimentally constrained parameters within their uncertainties (Table 1), and in W's from 0 to three times their nominal values move the phase boundaries by less than 0.4 X_{Fe} units. For all parameters except q of perovskite, the changes are less than 0.2 X_{Fe} units. Extreme variations in the F_o's, obtained by extrapolating their apparent temperature dependence (difference between low-T and high-T parameter sets) to 5000 K also fails to exclude the Earth from the perovskite stability field. A parametric phase diagram (Figure 10) shows that $MgSiO_3$ perovskite is stable for a wide range of thermal parameters. The stability limit of perovskite in this diagram lies close to the values of θ_o and γ_o adopted here, but outside their 1-σ uncertainty limits. The diagram illustrates an extreme lower bound on the stability of perovskite since temperatures at the top of D" and the average temperature over this layer are almost certainly well below 5000 K, possibly by as much as 2000 K. A temperature of 3000 K produces perovskite stability fields in Figures 8-10 which are 25-60 % wider. Alternative values of K_o and K_o' for perovskite [246 GPa, 4.5; *Yeganeh-Haeri et al.*, 1989] or the transformation of stishovite to its recently discovered high pressure form [*Tsuchida and Yagi*, 1989] have a much smaller effect than

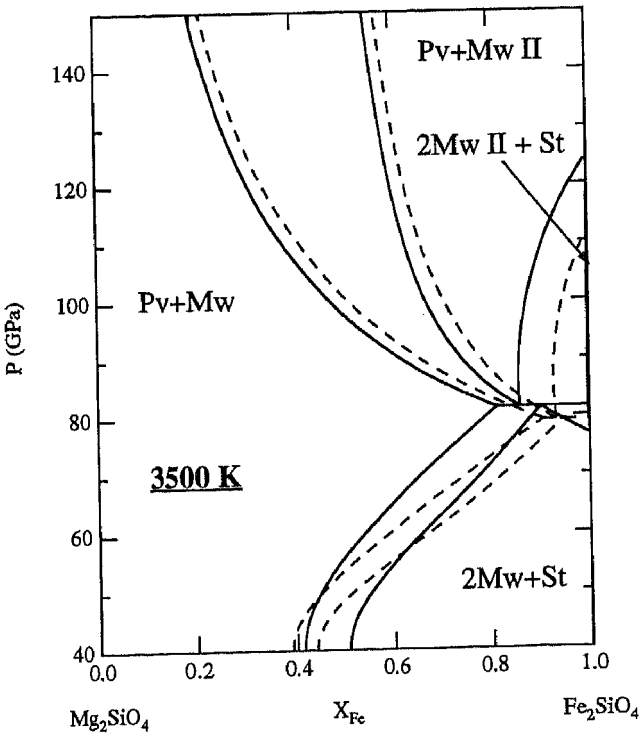

Fig. 8. High pressure orthosilicate phase diagram at 4000 K. Solid and dashed curves are calculated with the high temperature and global parameter sets respectively.

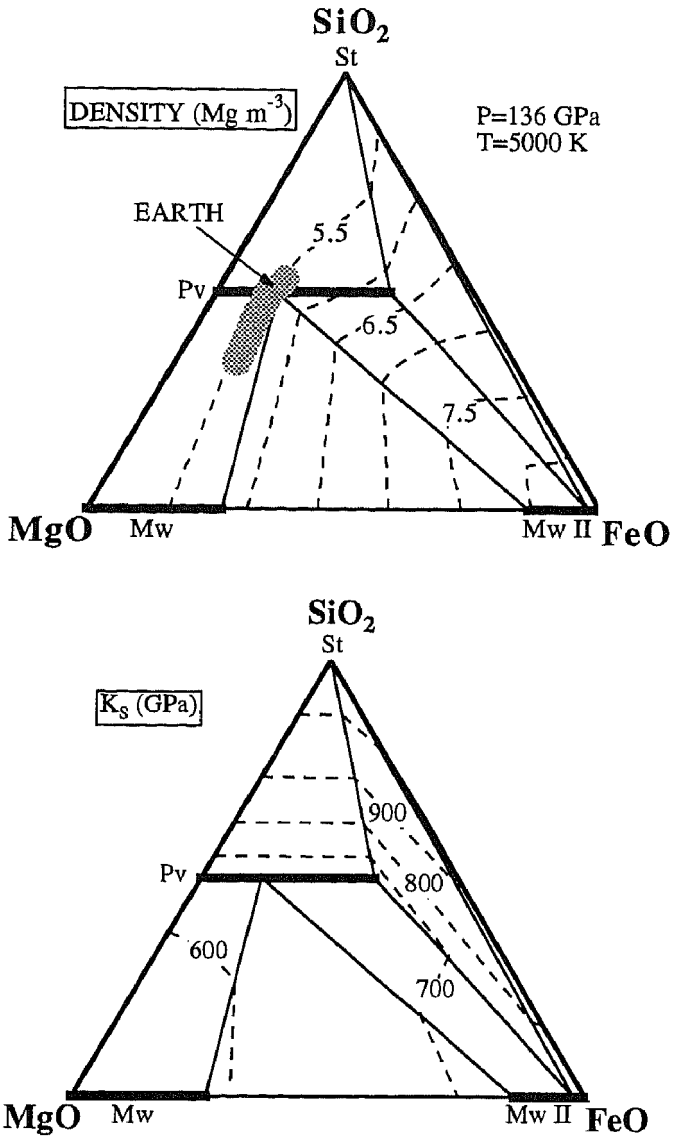

Fig. 9. Ternary MgO-FeO-SiO_2 phase diagram at 136 GPa and 5000 K calculated with the high temperature parameter set. Contours of density (upper figure) and adiabatic bulk modulus (lower figure) are superimposed. The shading, shown only in the upper figure for clarity, indicates the field of possible intersections of the contours corresponding to the observed density and adiabatic bulk modulus of the Earth allowed by uncertainties in calculated and seismically observed densities and bulk moduli. Adopting a value of 205 GPa for the room temperature phase transition in periclase eliminates Mw from the diagram and shifts the Pv+Mw II+St coexistence field towards lower iron contents (X_{Fe}(Pv)=0.58, X_{Fe}(Mw II)=0.83).

variations in thermal parameters on the location of the Earth and the position of phase boundaries on the diagram. Perhaps the largest uncertainty lies in the pressure of the assumed phase transition in periclase. The first principles calculations of *Bukowinski* [1985] provide a probable lower bound on the transition pressure of 205 GPa at 300 K, much lower than the value adopted here from more recent results [500 GPa, *Mehl et al.*, 1988; this value is also consistent with the results of *Agnon and Bukowinski*, 1990; and *Zhang and Bukowinski*, 1991 which are based on modified electron gas theories]. Adopting the lower value expands the Mw II+St field somewhat but not enough to encompass the Earth.

CONCLUSIONS

Our results indicate that the breakdown of (Mg,Fe)SiO_3 perovskite to its constituent oxides is unlikely in the Earth. If core-mantle boundary temperatures are much lower than those derived from shock wave experiments [*Williams et al.*, 1987; *Jeanloz*, 1990], several alternative explanations for the seismic reflectors at the base of the mantle are possible. Small amounts of stishovite may be responsible, from silica enrichment relative to metasilicate stoichiometry (Figure 9). The phase transition in magnesiowüstite to its high pressure form may produce anomalous velocity gradients near the core-mantle boundary, although it appears much too diffuse to produce a seismic discontinuity (Figure 8). Still unobserved

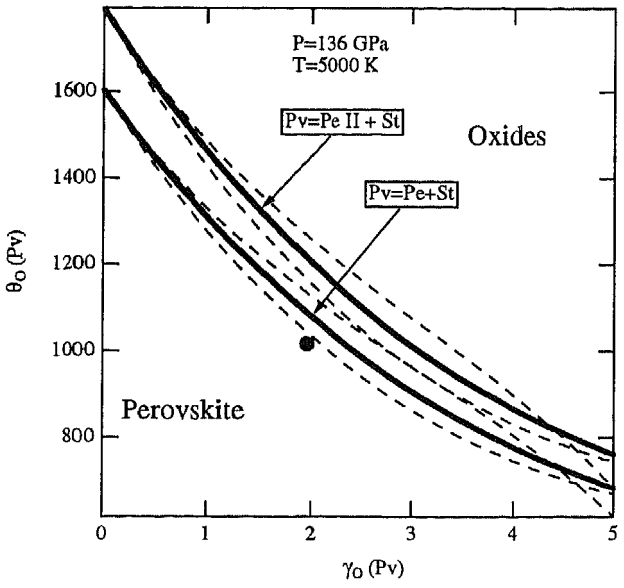

Fig. 10. Parametric phase diagram showing extreme lower bounds on the size of the stability field of $MgSiO_3$ perovskite relative to its constituent oxides at the pressure-temperature conditions of D''. The bold curves indicate the stability limit of perovskite for q(Pv)=2.5, while the lower and upper surrounding dashed lines show the limit for q(Pv)=1.5 and 3.5 respectively. The circle represents the best fitting values adopted here (Figure 3; and Table 1). The size of the symbol is comparable to the 1-σ uncertainties. Adopting different forms for the thermodynamic potentials (e.g. an Einstein model for the thermal energy) may lead to best fit values which fall outside our uncertainties. However, the position of the best fit values relative to the breakdown reactions is unlikely to change by more than a few percent in θ_o or 10 % in γ_o. Lowering the temperature to 3000 K increases the stability of perovskite and shifts the curves towards higher values of γ_o by 0.5.

phase transitions in calcic, diopsidic or $(Mg,Fe)SiO_3$ perovskite, including the predicted orthorhombic to cubic transition in the latter [*Wolf and Bukowinski*, 1985; *Bukowinski and Wolf*, 1988; see also *Hemley and Cohen*, 1992], may produce velocity discontinuities at the appropriate pressures. Partial reaction of Mg-rich perovskite with iron alloys, similar to that observed at lower pressures [*Knittle and Jeanloz*, 1989a, 1991a], may also produce seismic reflectors.

All of these explanations rely on perovskite dominated assemblages and thus cannot reconcile geotherms based on shock wave experiments with the lack of partial melt in D". The melting point of iron under shock loading, and in static compression experiments at lower pressures is currently a matter of active debate [*Ross et al.*, 1990; *Boehler et al.*, 1990]. However, if the shock wave data and the predicted perovskite melting curve are approximately correct, they require either the absence of Mg-rich perovskite from D" or a substantial change in its properties, probably much greater than that associated with the predicted orthorhombic to cubic phase transformation. An exotic bulk composition in D", perhaps dominated by Ca and Al oxide components [*Ruff and Anderson*, 1980], may be required. Alternatively, a breakdown or transformation of $(Mg,Fe)SiO_3$ perovskite to a more diverse assemblage than those considered here remains a possible explanation of the seismic reflectors and the absence of melt in D". Consideration of other chemical components may lower the free energy of the non-perovskite assemblage, inducing a breakdown to a mixture of oxides and metallic alloys (Fe, FeSi). Though speculative, a metallic alloy-oxide layer may be heterogeneous on many length scales because of the disparate physical properties of the two components [*Knittle and Jeanloz*, 1991a]. This provides a possible explanation for observed heterogeneity in D" on length scales ranging from the smallest observable with seismic probes (100 km, roughly one seismic wavelength) to nearly the diameter of the core [*Lavely et al.*, 1986; *Creager and Jordan*, 1986; *Morelli and Dziewonski*, 1987; *Young and Lay*, 1987; *Weber and Körnig*, 1990;].

Acknowledgments. We thank C. Lithgow-Bertelloni and two anonymous reviewers for helpful comments on the manuscript. This work supported by NSF grant EAR-8816819.

REFERENCES

Agnon, A., and M.S.T. Bukowinski, Thermodynamic and elastic properties of a many-body model for simple oxides, *Phys. Rev. B, 41*, 7755-7766, 1990.

Akimoto, S., High-pressure research in geophysics: Past, present and future in *High Pressure Research in Mineral Physics*, edited by M.H. Manghnani and Y. Syono, Terra Scientific Publishing Company, Tokyo, American Geophysical Union, Washington, 1987.

Ashcroft, N.W., and N.D. Mermin, *Solid State Physics*, Saunders College, Philadelphia, 1976.

Ashida, T., S. Kume, and E. Ito, Thermodynamic aspects of phase boundary among α, β, and γ Mg_2SiO_4 in *High Pressure Research in Mineral Physics* , edited by M. H. Manghnani and Y. Syono, pp. 427-438, TERRAPUB/AGU, Tokyo/Washington, 1987.

Ashida, T., S. Kume, E. Ito, and A. Navrotsky, $MgSiO_3$ ilmenite: Heat capacity, thermal expansivity, and enthalpy of transformation, *Phys. Chem. Min., 16*, 239-245, 1988.

Bass, J.D., R.C. Liebermann, D.J. Weidner, and S.J. Finch, Elastic properties from acoustic and volume compression experiments, *Phys. Earth Planet. Int., 25*, 140-158, 1981.

Bass, J.D., and M. Kanzaki, Elasticity of a majorite-pyrope solid solution, *Geophys. Res. Lett., 17*, 1989-1992, 1990.

Bloxham, J., and A. Jackson, Fluid flow near the surface of Earth's outer core, *Revs. Geophys.*, 29, 97-120.

Boehler, R., N.V. von Bargen, A. Chopelas, Melting, thermal expansion, and phase transition of iron at high pressures, *J. Geophys. Res., 95*, 21731-21736, 1990.

Boyd, R.F., J.R. England, and B.T. Davis, Effects of pressure on the melting and polymorphism of enstatite, $MgSiO_3$, *J. Geophys. Res., 69*, 2101-2109, 1964.

Brown, M.J., and R.G. McQueen, The equation of state for iron and the Earth's core, in *High Pressure Research in Geophysics*, edited by S. Akimoto and M.H. Manghnani, Center for Academic Publications, Tokyo, 611-623, 1982.

Bukowinski, M.S.T., First principles equations of state of MgO and CaO, *Geophys. Res. Lett., 12*, 536-539, 1985.

Bukowinski, M.S.T., and G.H. Wolf, Equation of state and possible critical phase transitions in $MgSiO_3$ perovskite at lower-mantle conditions, in *Structural and Magnetic Phase Transitions in Minerals*, edited by S. Ghose, J.M.D. Coey, and E. Salje, pp. 91-112, Springer-Verlag, New York, 1988.

Bukowinski, M.S.T., and G.H. Wolf, Thermodynamically consistent decompression: Implications for lower mantle composition, *J. Geophys. Res., 95*, 12583-12593, 1990.

Callen, H.B., *Thermodynamics and an Introduction to Thermostatistics*, 2nd ed., 493 pp., John Wiley, New York, 1985.

Courtillot, V., and J. Besse, Magnetic field reversals, polar wander, and core-mantle coupling, *Science, 237*, 1140-1147, 1987.

Creager, K.C., and T.J. Jordan, Aspherical structure of the core-mantle boundary from PKP travel times, *Geophys. Res. Lett., 13*, 1497-1500, 1986.

Duffy, T. S., and D. L. Anderson, Seismic velocities in mantle minerals and the mineralogy of the upper mantle, *J. Geophys. Res., 94*, 1895-1912, 1989.

Duncan, R.A., and M.A. Richards, Hotspots, mantle plumes, flood basalts, and true polar wander, *Revs. Geophys., 29*, 31-50, 1991.

Dziewonski, A.M., and D.L. Anderson, Preliminary reference Earth model, *Phys. Earth Planet. Int., 25*, 297-356, 1981.

Fei, Y., H. Mao, and B.O. Mysen, Experimental determination of element partitioning and calculation of phase relations in the MgO-FeO-SiO_2 system at high pressure and high temperature, *J. Geophys. Res., 96*, 2157-2170, 1991a.

Fei, Y., H.K. Mao, J. Shu, G. Parthasarathy, and W.A. Bassett, Simultaneous high P-T x-ray diffraction study of β-$(Mg,Fe)_2SiO_4$ to 26 GPa and 900 °K, *J. Geophys. Res., 97*, 4489-4495, 1992.

Gasparik, T., Phase relations in the transition zone, *J. Geophys. Res., 95*, 15751-15769, 1990.

Graham, E., and G. Barsch, Elastic constants of single-crystal forsterite as a function of temperature and pressure, *J. Geophys. Res., 74*, 5949-5960, 1969.

Graham, E., J. Schwab, S. Sopkin, and H. Takei, The pressure and temperature dependence of the elastic properties of single-crystal fayalite Fe_2SiO_4, *Phys. Chem. Minerals, 16*, 186-198, 1988.

Guggenheim, E.A., *Mixtures*, 270 pp., Clarendon, Oxford, 1952.

Hazen, R.M., J. Zhang, and J. Ko, Effects of Fe/Mg on the compressibility of synthetic wadsleyite: β-$(Mg_xFe_{1-x})_2SiO_4$ ($x<0.25$), *Phys. Chem. Minerals, 17*, 416-419, 1990.

Hemley, R.J., and R.E. Cohen, Silicate perovskite, *Annu. Revs. Earth Planet. Sci., 20*, 553-600, 1992.

Hemley, R.J., L. Stixrude, Y. Fei, H.K. Mao, Constraints on lower

mantle composition from P-V-T measurements of (Fe,Mg)SiO_3 perovskite and (Fe,Mg)O magnesiowüstite, in *High Pressure Research: Application to Earth and Planetary Sciences* edited by Y. Syono and M.H. Manghnani, TERRAPUB, Tokyo, in press, 1992.

Isaak, D.G., O. Anderson, and T. Goto, Elasticity of single-crystal forsterite measured to 1700° K, *J. Geophys. Res., 94*, 5895-5906, 1989.

Ita, J.J., and L. Stixrude, Petrology, elasticity and composition of the transition zone, *J. Geophys. Res., 97*,.6849-6866, 1992.

Ito, E., and E. Takahashi, Postspinel transformations in the system Mg_2SiO_4-Fe_2SiO_4 and some geophysical implications, *J. Geophys. Res., 94*, 10637-10646, 1989.

Ito, E., and T. Katsura, Melting of iron-silicate systems, *Union Program and Abstracts, XX General Assembly, International Union of Geodesy and Geophysics*, pg. 119, 1991.

Jackson, I., S.K. Khana, A. Revcolevschi, J. Berthon, Elasticity and polymorphism of wüstite $Fe_{1-x}O$, *J. Geophys. Res., 95*, 21671-21685, 1990.

Jackson, I., and H. Niesler, The elasticity of periclase to 3 GPa, and some geophysical implications, in *High Pressure Research in Geophysics*, edited by S. Akimoto and M.H. Manghnani, pp. 93-113, Center for Academic Publications, Tokyo, 1982.

Jeanloz, R., Universal equation of state, *Phys. Rev. B, 38*, 805-807, 1988.

Jeanloz, R., Shock wave equation of state and finite strain theory, *J. Geophys. Res., 94*, 5873-5886, 1989.

Jeanloz, R., The nature of the Earth's core, *Annu. Rev. Earth Planet. Sci., 18*, 357-386, 1990.

Jeanloz, R., and T.J. Ahrens, Equations of state of FeO and CaO, *Geophys. J.R. Astron. Soc.*, 62, 505-528, 1980.

Jeanloz, R., and A.B. Thompson, Phase transitions and mantle discontinuities, *Revs. Geophys. Space Phys., 21*, 51-74, 1983.

Jeanloz, R., and E. Knittle, Density and composition of the lower mantle, *Philos. Trans. R. Soc. London, Ser. A, 328*, 377-389, 1989.

Katsura, T., and E. Ito, The system Mg_2SiO_4-Fe_2SiO_4 at high pressures and temperatures: Precise determination of stabilities of olivine, modified spinel, and spinel, *J. Geophys. Res., 94*, 15663-15670, 1989.

Knittle, E., and R. Jeanloz, High pressure metallization of FeO and implications for the Earth's core, *Geophys. Res. Lett.., 13*, 1541-1544, 1986.

Knittle, E., and R. Jeanloz, Synthesis and equation of state of (Mg,Fe)SiO_3 perovskite to over 100 gigapascals, *Science, 235*, 668-670, 1987.

Knittle, E., and R. Jeanloz, Melting curve of (Mg,Fe)SiO_3 perovskite to 96 GPa: Evidence for a structural transition in lower mantle melts, *Geophys. Res. Lett., 16*, 421-424, 1989a.

Knittle, E., and R. Jeanloz, Simulating the core-mantle boundary: An experimental study of high-pressure reactions between silicates and liquid iron, *Geophys. Res. Lett., 16*, 609-612, 1989b.

Knittle, E., and R. Jeanloz, Earth's core-mantle boundary: Results of experiments at high pressures and temperatures, *Science, 251*, 1438-1443, 1991a.

Knittle, E., and R. Jeanloz, The high-pressure phase diagram of $Fe_{0.94}O$: A possible constituent of the Earth's core, *J. Geophys. Res., 96*, 16169-16180, 1991b.

Knittle, E., R. Jeanloz, and G.L. Smith, Thermal expansion of silicate perovskite and stratification of the Earth's mantle, *Nature, 319*, 214-216, 1986.

Knopoff, L., and J.N. Shapiro, Comments on the interrelationships between Grünesien's parameter and shock and isothermal equations of state, *J. Geophys. Res., 74*, 1439-1450, 1969.

Krupka, K. M., B. S. Hemingway, R. A. Robie, and D. M. Kerrick, High temperature heat capacities and derived thermodynamic properties of anthophyllite, diopside, dolomite, enstatite, bronzite, talc, tremolite, and wollastonite, *Am. Mineral., 70*, 261- 271, 1985.

Krupka, K. M., R. A. Robie, and B. S. Hemingway, High temperature heat capacities of corundum, periclase, anorthite, $CaAl_2Si_2O_8$ glass, muscovite, pyrophyllite, $KAlSi_3O_8$ glass, grossular, and $NaAlSi_3O_8$ glass, *Am. Mineral., 64*, 86-101, 1979.

Lange, R., and I.S.E. Carmichael, Densities of Na_2O-K_2O-CaO-MgO-FeO-Fe_2O_3-Al_2O_3-TiO_2-SiO_2 liquids: New measurements and derived partial molar properties, *Geochim Cosmochim. Acta, 51*, 2931-3946, 1987.

Lavely, E.M., D.W. Forsyth, and P. Friedemann, Scales of heterogeneity at the core-mantle boundary, *Geophys. Res. Lett., 13*, 1505-1508, 1986.

Liebermann, R.C., Elasticity of olivine (α), beta (β), and spinel (γ) polymorphs of germanates and silicates, *Geophys. J.R. astr. Soc., 42*, 899-929, 1975.

Mao, H.K., R.J. Hemley, Y. Fei, J.F. Shu, L.C. Chen, A.P. Jephcoat, Y. Wu, and W.A. Bassett, Effect of pressure, temperature and composition on lattice parameters and density of (Fe,Mg)SiO_3 perovskites to 30 GPa, *J. Geophys. Res., 96*, 8069-8080, 1991.

McQueen, R.G., S.P. Marsh, J.W. Taylor, J.N. Fritz, and W.J. Carter, The equation of state of solids from shock wave studies, in *High Velocity Impact Phenomena*, edited by R. Kinslow, pp. 294-419, Academic, San Diego, 1970.

Mehl, M.J., R.E. Cohen, and H. Krakauer, Linearized augmented plane wave electronic structure calculations for MgO and CaO, *J. Geophys. Res., 93*, 8009-8022, 1988.

Morelli, A., and A.M. Dziewonski, Topography of the core-mantle boundary and lateral homogeneity of the liquid core, *Nature, 325*, 678-683, 1987.

Ohtani, E., and M. Kumazawa, Melting of forsterite Mg_2SiO_4 up to 15 GPa, *Phys. Earth Planet. Int., 27*, 32-38, 1981.

Olinger, B., Compression studies of forsterite (Mg_2SiO_4) and enstatite ($MgSiO_3$), in *High Pressure Research: Applications in Geophysics*, edited by M.H. Manghnani and S. Akimoto, pp. 255-266, Academic, San Diego, 1977.

Presnall, D.C., and T. Gasparik, Melting of enstatite ($MgSiO_3$) from 10 to 16.5 GPa and forsterite (Mg_2SiO_4)-Majorite ($MgSiO_3$) eutectic at 16.5 GPa: Implications for the origin of the mantle, *J. Geophys.. Res., 95*, 15771-15777, 1990.

Ross, M., D.A. Young, R. Grover, Theory of the iron phase diagram at Earth core conditions, *J. Geophys. Res., 95*, 21713-21716, 1990.

Ruff, L., and D.L. Anderson, Core formation, evolution, and convection: A geophysical model, *Phys. Earth Planet. Int., 21*, 181-201, 1980.

Sawamoto, H., D. Weidner, S. Sasaki, and M. Kumazawa, Single-crystal elastic properties of the modified spinel (beta) phase of Mg_2SiO_4, *Science, 224*, 749-751, 1984.

Sawamoto, H., M. Kozaki, A. Jujimura, and T. Akamatsu, Precise measurement of compressibility of γ-Mg_2SiO_4 using synchrotron radiation, paper presented at 27th High Pressure Conference Sapporo, Japan, 1986.

Shapiro, J.N., and L. Knopoff, Reduction of shock-wave equations of state to isothermal equations of state, *J. Geophys. Res., 74*, 1435-1438, 1969.

Stebbins, J.F., I.S.E. Carmichael, and L.K. Moret, Heat capacities and entropies of silicate liquids and glasses, *Contrib. Mineral. Petrol., 86*, 131-148, 1984.

Stixrude, L., and M.S.T. Bukowinski, Fundamental thermodynamic relations and silicate melting with implications for the constitution of D'', *J. Geophys. Res., 95*, 19311-19325. 1990.

Suzuki, I., Thermal expansion of olivine and periclase and their anharmonic properties, *J. Phys. Earth , 25*, 145-159, 1975a.

Suzuki, I., Cell parameters and linear thermal expansion coefficients of orthopyroxenes, *J. Seismol. Soc. Jpn., 28*, 1-9, 1975b.

Suzuki, I., Thermal expansion of γ- Mg_2SiO_4 , *J. Phys. Earth, 27*, 53-61, 1979.

Suzuki, I., and O. L. Anderson, Elasticity and thermal expansion of a natural garnet up to 1000 K, *J. Phys. Earth., 31*, 125-138, 1983.

Suzuki, I., E. Ohtani, and M. Kumazawa, Thermal expansion of modified spinel, β–Mg_2SiO_4, *J. Phys. Earth, 28*, 273-280, 1980.

Suzuki, I., K. Seya, H. Takei, and Y. Sumino, Thermal expansion of fayalite, *Phys. Chem. Minerals*, *7*, 60-63, 1981.

Tarduno, J.A., W.V. Sliter, L. Kroenke, M. Leckie, H. Mayer, J.J. Mahoney, R. Musgrave, M. Storey, and E.L. Winterer, Rapid formation of the Ontong Java plateau by Aptian mantle plume volcanism, *Science, 254*, 399-403, 1991.

Touloukian, Y. S., R. S. Kirby, R. E. Taylor, and T. Y. R. Lee, in *Thermal Expansion, Nonmetallic Solids*, 1658 pp., TPRC 13, IFI/Plenum, New York, 1977.

Tsuchida, Y., and T. Yagi, A new post-stishovite high pressure polymorph of silica, *Nature, 340*, 217-220, 1989.

Wallace, D.C., *Thermodynamics of Crystals*, John Wiley, New York, 1972.

Watanabe, H., Thermochemical properties of synthetic high-pressure compounds relevant to the Earth's mantle, in *High Pressure Research in Geophysics*, edited by S. Akimoto and M. H. Manghnani, pp. 93-113, Center for Academic Publications, Tokyo, 1982.

Weber, M., and M. Körnig, Lower mantle inhomogeneities inferred from PcP precursors, *Geophys. Res. Lett., 17*, 1993-1996, 1990.

Weidner, D.J., H. Wang, and J. Ito, Elasticity of orthoenstatite, *Phys. Earth Planet. Int., 17*, P7-P13, 1978.

Weidner, D.J., J.D. Bass, A.E. Ringwood, and W. Sinclair, The single-crystal elastic moduli of stishovite, *J. Geophys. Res., 87*, 4740-4746, 1982.

Weidner, D.J., H. Sawamoto, and S. Sasaki, Single-crystal elastic properties of the spinel phase of Mg_2SiO_4, *J. Geophys. Res., 89*, 7852-7859, 1984.

Weidner, D.J., and E. Ito, Elasticity of $MgSiO_3$ in the ilmenite phase, *Phys. Earth Planet. Int., 40*, 65-70, 1985.

Williams, Q., R. Jeanloz, J. Bass, B. Svendsen, T.J. Ahrens, The melting curve of iron to 250 Gigapascals: A constraint on the temperature at Earth's center, *Science, 236*, 181-182, 1987.

Williams, Q., E. Knittle, R. Reichlin, S. Martin, and R. Jeanloz, Structural and electronic properties of Fe_2SiO_4-fayalite at ultrahigh pressures: amorphization and gap closure, *J. Geophys. Res., 95*, 21549-21564, 1990.

Williams, Q., and R. Jeanloz, Melting relations in the iron-sulfur system at ultra-high pressures: Implications for the thermal state of the Earth, *J. Geophys. Res., 95*, 19299-19310, 1990.

Wolf, G.H., and M.S.T. Bukowinski, Ab initio structural and thermoelastic properties of orthorhombic $MgSiO_3$ perovskite, *Geophys. Res. Lett., 12*, 809-812, 1985.

Wood, B.J., and D.G. Fraser, *Elementary Thermodynamics for Geologists*, 303 pp., Oxford University Press, 1977.

Yeganeh-Haeri, A., D.J. Weidner, and E. Ito, Single crystal elastic moduli of magnesium metasilicate perovskite, in *Perovskite: A Structure of Great Interest to Geophysics and Materials Science*, edited by A. Navrotsky and D.J. Weidner, pp. 13-26, Terra Scientific Publishing Company, Tokyo, American Geophysical Union, Washington, 1989.

Young, C.J., and T. Lay, The core-mantle boundary, *Annu. Rev. Earth Planet. Sci., 15*, 25-46, 1987.

Zhang, H., and M.S.T. Bukowinski, Modified potential-induced-breathing model of the potential between closed-shell ions, *Phys. Rev. B, 44*, 2495-2503, 1991.

L. Stixrude, Geophysical Laboratory, Carnegie Institution of Washington, 5251 Broad Branch Rd. NW, Washington, DC 20015.

M.S.T. Bukowinski, Dept. of Geology and Geophysics, University of California, Berkeley, CA 94720.